Zanco Journal of Human Sciences (ZJHS)

TYPE: Original article
DOI https://doi.org/10.21271/zjhs.30.SpB.31

Monitoring LULC Changes in the Semi-Mountainous Region of Duhok Governorate Utilising Landsat Imagery and SVM

OPEN ACCESS
*Corresponding author
Dastan Fathi Ahmed
dastan.fa6323@stu.uod.ac

Dastan Fathi Ahmed/ Department of Geography, College of Humanities, University of Duhok, Duhok, Kurdistan Region, Iraq

Nashwan Shukri Abdullah/ Department of Geography, College of Humanities, University of Duhok, Duhok, Kurdistan Region, Iraq

RECEIVED :11 /10/2025
ACCEPTED :15/12/ 2025
PUBLISHED :15/04/ 2026

Abstract

This study analyses long-term changes in land use and land cover (LULC) in the semi-mountainous region of Dohuk Governorate in the Kurdistan Region of Iraq during the period 2000-2023, utilising Landsat satellite imagery (Landsat 5 TM and Landsat 8 OLI), and Machine Learning (ML) classification techniques. The terrain of the study area is characterised by an intertwined landscape, combining plateaus and agricultural plains. This creates spectral challenges in distinguishing between similar land categories and makes the area an ideal model for testing the effectiveness of ML algorithms in complex environments.

Using the ArcGIS 3.5 environment, supervised classification was performed employing a support vector machine (SVM) algorithm. The results demonstrated clear changes in LULC patterns, with the planted/cultivated category increasing from 26.5% to 31.3%. The developed area also increased from 3.5% to 7.4%, while barren land decreased from 42.1% to 35%. Overall classification accuracies were 99.04% for 2000 and 97.10% for 2023, with Kappa values of 0.9868 and 0.9609, respectively, indicating high classification performance. Major LULC changes that occurred in the study are, including the conversion of large areas of barren to planted/cultivated and herbaceous categories, reflecting the effects of urban expansion and unsustainable land use in the study area.

Keywords:
Land Use /Land Cover (LULC); Remote Sensing (RS); Machine-Learning (ML); Support Vector Machine (SVM), Duhok governorate

1. Introduction

The changes in Land Use/ Land Cover in the contemporary world have become a real challenge (Bhagawat 2011). reflecting the dynamic interaction between anthropogenic activities and natural processes. LULC are two elements that have been the focus of separate research for a while (OĞUZ, Hassan, & Omar 2024). Monitoring LULC is essential for evaluating the land surface, which is influenced by climatic events, human interventions, and natural disasters. Understanding LULC requires perceiving the Earth as a system of interdependent components and processes, or as a spatial and dynamic phenomenon (Aspinall & Hill 2007).

As a methodological approach, the detection of change focuses on analysing variations in radiance between multi-temporal satellite images, in order to localise and quantify changes in land cover (Lunetta et al. 2004) Change detection technique allows both positive developments and negative impacts, such as land degradation and loss of productivity, to be identified (Basseville 2009). Studying the patterns of LULC changes provides crucial information for simulating spatial and temporal dynamics and understanding their environmental influences.

Classification techniques categorise pixels within an image, with each group representing a specific class of land cover (Bechtel & Daneke 2012; Abburu & Golla 2015). Classifiers represent a contemporary approach to land cover classification, emerging from numerical methods to identify patterns in parametric and non-parametric techniques (Phiri & Morgenroth 2017). Conversely, traditional parametric methods (e.g. maximum likelihood classification and minimum distance) are predicated on statistical assumptions, including the assumption of a normal distribution of data.

The typical applications of the conventional approaches to non-parametric supervised ML classifiers include SVM, artificial neural networks (ANN), K-nearest neighbour (KNN), decision trees, and random forests (RF) (Adam et al. 2014; Thanh & Kappas 2017; Maxwell et al. 2018; Ge et al. 2020; Ghayour et al. 2021; Tariq et al. 2023; Liang et al. 2023; Amini et al. 2022). The development of both parametric and non-parametric classifiers has led to the question of which classification technique should be chosen to provide the intended results. This has given rise to comparative studies of different classifiers for land cover classification. A number of the aforementioned studies have relied on unsupervised classification techniques (Tarabalka et al. 2009), whilst others have employed supervised classification methods (Zhang et al. 2012). Some studies have also addressed semi-classification methods (Xia et al. 2014).

ML is a branch of artificial intelligence that enables computer systems to learn from information and data and identify patterns with minimal human intervention, and is therefore a powerful tool for large-scale environmental analysis (Zhang & Li 2022). Among various ML approaches, Support Vector Machines (SVM) have gained popularity due to their ability to handle complex classification tasks and produce reliable results, even with limited training data. It has shown competitive performance when applied in LULC studies to distinguish between different types of land cover (Alam et al. 2025; Aljanabi, Dedeoğlu, & Şeker 2024).

Based on these developments, combining RS with geospatial technologies and machine learning (ML) models has improved the accuracy and efficiency of land cover mapping (Debebe et al. 2023). Although the SVM algorithm has been widely used in LULC classification studies in various regions around the world, its application in semi-mountainous environments within the Dohuk Governorate has not been addressed in previous literature. Therefore, this study is the first to employ SVM technology in this region between 2000 and 2023.

Between 1998 and 2011, the study area experienced rapid and uncontrolled urban growth, which resulted in negative environmental impacts and a considerable reduction in open spaces (Jambally 2013). Since 2003, the growth in population and the lack of effective urban planning regulations have contributed to a considerable increase in built-up areas, accompanied by a corresponding decline in dry vegetation. By 2014, the situation was exacerbated by an influx of refugees fleeing political instability in neighbouring regions, which led to intensified population expansion and increased pressure on land resources (UN-Habitat 2020) Consequently, agricultural land has expanded at the expense of forests and grasslands, and the growth of plants in lowland areas has been affected negatively by both urbanisation and resource extraction (Mzuri, et al. 2021).

The first objective of this study is to analyse the spatial and temporal changes in LULC patterns in the study area during the period 2000-2023 using satellite data and GIS techniques. The second is to classify LULC into specific categories (e.g., urban areas, agricultural lands, forests, barren lands) using the SVM algorithm. The third is to evaluate the effectiveness of RS and GIS techniques in detecting and analysing long-term environmental changes in semi-mountainous regions.

The study hypotheses are (1) To what extent has Dohuk Governorate experienced transformations in LULC patterns during the period 2000–2023? (2) How effective are remote sensing data and GIS techniques in detecting environmental changes and identifying areas that should be prioritised for environmental protection?

2. Methodology and Data Collection

2.1 Study Area

The study area is geographically delineated by the natural boundaries of a semi-mountainous region situated within the administrative limits of the Dohuk Governorate, located in the extreme north-west of the Kurdistan Region of Iraq. It is bordered by Erbil Governorate to the east and south-east, Nineveh Governorate to the south-west, and the international border with Syria to the west. The total area encompasses approximately 4,248 km², representing 39 per cent of the overall area of Dohuk Governorate. The northern extent of the study area comprises complex and indistinct natural features that overlap with the mountainous terrain of the governorate. In order to define and distinguish this boundary, a series of carefully considered procedures were employed, based on specific criteria including elevation, river basin morphology, and the conceptual framework of semi-mountainous landscapes. Geospatially, the study area lies between latitudes 37°06′N and 38°10′N, and longitudes 42°47′E and 44°13′E, corresponding to Zone 38N of the Universal Transverse Mercator (UTM) coordinate system (WGS84) Fig (1). Between 2000 and 2023, the region experienced average annual rainfall ranging from 200 to 500 millimetres, while the mean annual temperature during this period was 27.2 °C. The geology of the study area exemplifies the characteristics of the 'unstable shelf' located between the Arabian and Anatolian tectonic plates (Jassim & Buday 2006). The region is defined by two bands of unstable shelf mass that run parallel to the Mesozoic margin of the Arabian Plate and the Late Cretaceous foreland basin (Fouad 2015). Topographically, the study area exhibits a gradual elevation gradient from north to south. Elevations in the northern sector range between 682 and 1,051 metres above sea level, while the southern regions descend to altitudes of approximately 222 to 363 metres. Additionally, isolated elevated points are sporadically distributed across the eastern and southern parts of the study area.

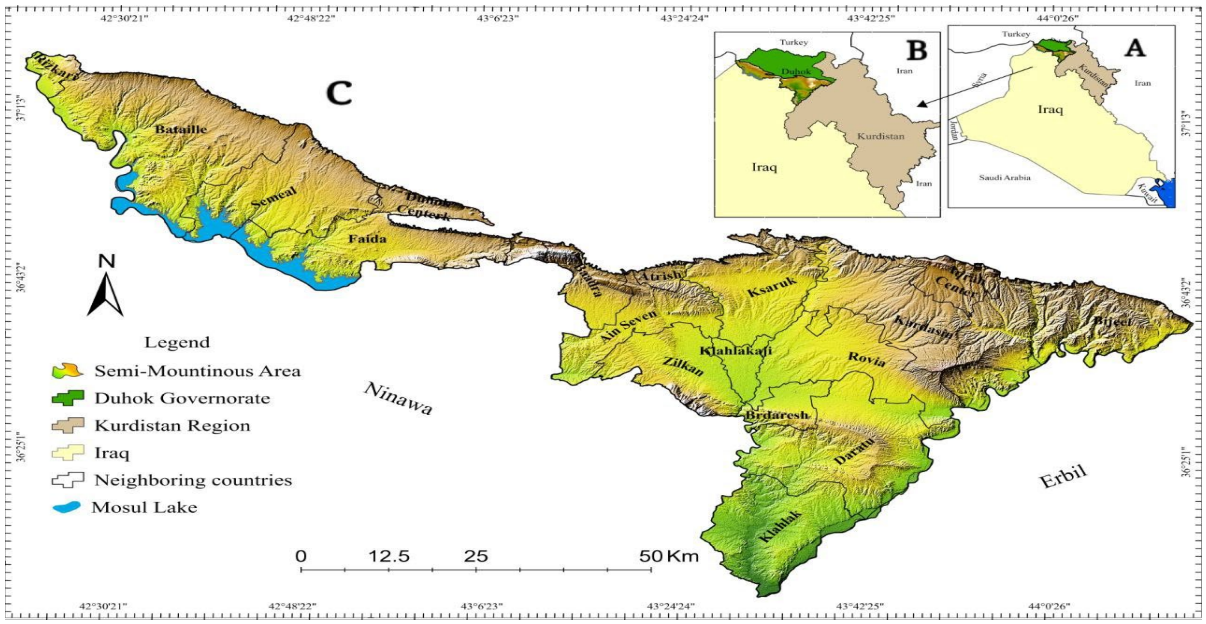

Fig. 1. The Semi-Mountainous Area Extent of Duhok Governorate with Elevation Feature. **(A)** Study location from the borders of Iraq, **(B)** Study location from the borders of the Kurdistan Region of Iraq, **(C)** Study area.

2.2 Satellite Data

Landsat 5 Thematic Mapper (TM) and Landsat 8 Operational Land Imager (OLI) Level-2 surface reflectance products, obtained from the USGS Earth Explorer platform, were used in this study at 30m spatial resolution. These datasets, processed by NASA, include radiometric calibration (Level 1) and atmospheric correction (Level 2). Image selection was based on the seasonal climatic conditions of the study area, with dry and wet seasons influencing land surface visibility (Gaznayee et al. 2022). To ensure temporal consistency, images were chosen from similar dates between 2000 and 2023, primarily in May, when atmospheric clarity is highest. The selected scenes supported the extraction and quantification of LULC metrics. As illustrated in Table (1) and Fig. (2). the Google Earth image was also used to assess the classified LULC maps accurately.

Table *1*. Descriptions of the Landsat image used in this study

Year	Satellite	Acquisition date day /month	Sensor	Path/Row
2000	LANDSAT 5	10 May	TM	169/035
		17 May		170/053
		17 May		169/034
2023	LANDSAT 8	9 May	OLI	170/034
		10 May		169/035
		17 May		170/035

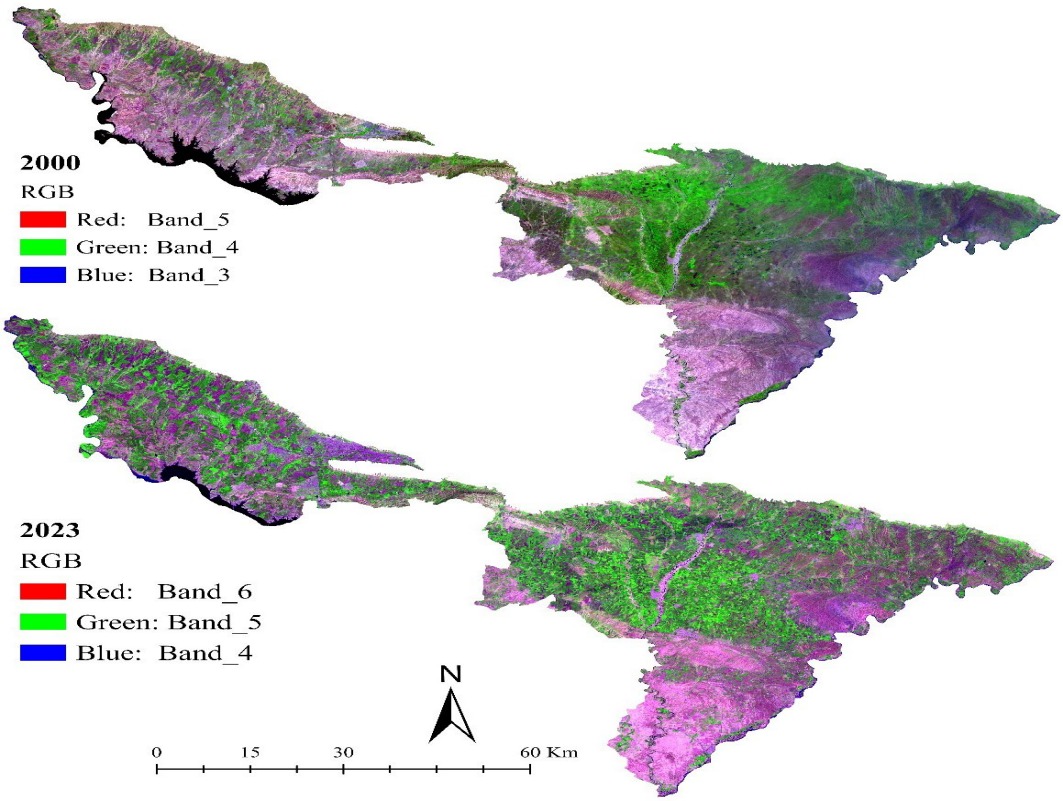

Fig 2. Multi-Temporal RGB Composites of the Study Area Using Landsat 5 TM (2000) & Landsat 8 OLI (2023) Imagery.

2.3 Methodological Framework for LULC Classification

To classify LULC categories from satellite imagery in this study, ArcGIS Pro 3.5 was employed. The classification followed the Level I scheme of the National Land Cover Database (NLCD), originally developed by Anderson (1971). This scheme was selected due to its compatibility with Landsat imagery, as it was specifically designed to accommodate the spatial and spectral characteristics of Landsat sensors (Anderson et al. 1976). The classification of LULC in the study area consists of six basic classes (Water, Developed, Barren, Forest, Herbaceous, Planted/Cultivated). Table (2). The workflow diagram of the methodology deployed in the study can be illustrated in Fig.3.

Table 2. LULC Classification Scheme (Adapted & modified from NLCD 2011)

Classification Scheme		General Description	Code
1	Water	Areas of open water	10
2	Developed	These areas contain a diverse range of building materials, ranging from residential gardens to urban areas with diverse population densities.	20
3	Barren	Areas of land with a rocky, sandy, or clayey composition that have almost no vegetation cover.	30
4	Forest	Areas are densely covered by trees, whether deciduous, evergreen, or mixed.	40
5	Herbaceous	Areas are dominated by grasses or herbaceous vegetation, generally greater than 80% of total vegetation. These areas are not subject to intensive management activities, such as tilling, but can be utilised for pastoral purposes.	70
6	Planted/Cultivated	Land that has been cultivated with crops or designated for grazing and forage production.	80

In this study, in order to organise tables and facilitate the presentation of results in graphs and figures, a set of abbreviations was adopted to refer to LULC classes. These letters were chosen based on the first letter of each LULC class name, as follows: (W) for water, (D) for developed areas, (B) for barren areas, (F) for forests, (H) for herbaceous, and (P/C) for planted/cultivated.

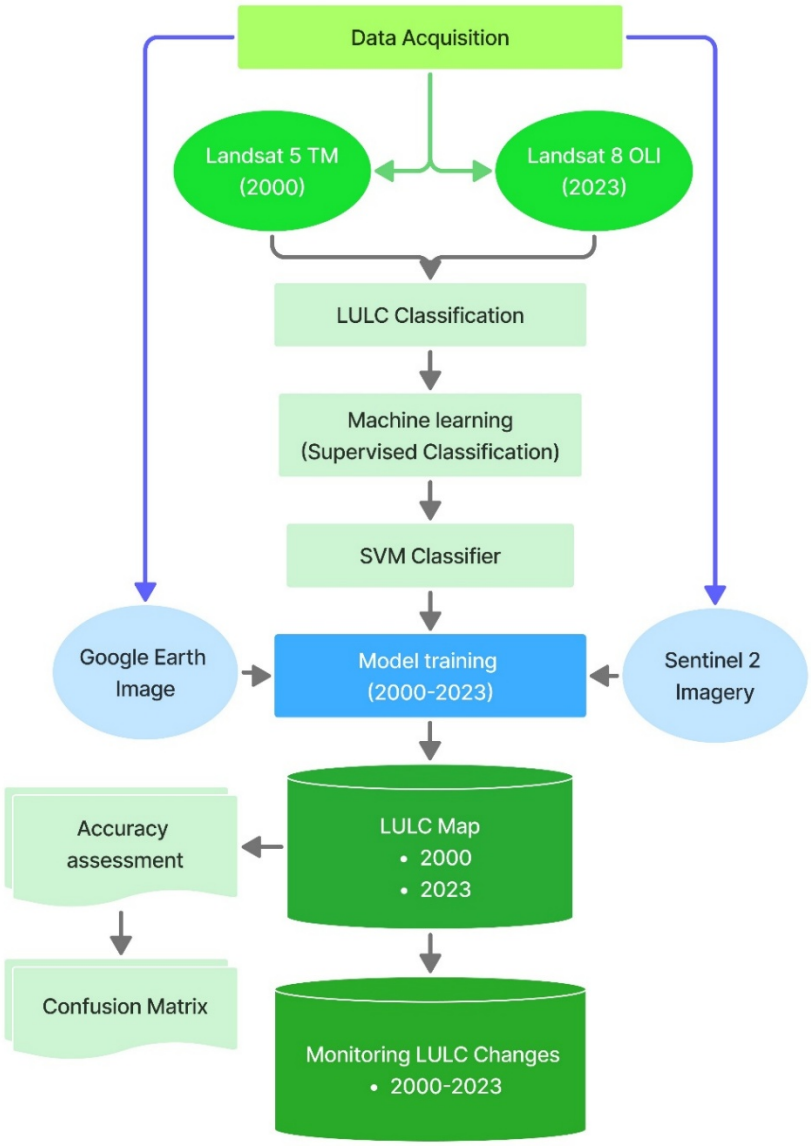

Fig 3. Workflow Diagram of the methodology deployed in the study.

2.3.1. Mapping LULC with a Machine learning approach

1. Classification Techniques for LULC Mapping

Machine learning is a technology that falls within the scope of artificial intelligence (AI) to analyse data. This technology is based on the basic idea that computer systems can learn from data typically provided and labeled by humans, in order to recognise patterns and make decisions with minimal human intervention during the prediction or inference phase (Zhang & Li 2022).

The advent of a variety of geospatial technologies, in combination with ML algorithms, has led to a revolution in environmental observation, allowing for more timely and accurate data on land cover dynamics (Debebe et al. 2023). This approach has become popular for the large-scale analysis of data with complexity, allowing for more accurate results and maps of LULC (Zhang & Li 2022).

A variety of ML approaches are available in the field of LULC mapping, such as random forest (RF), support vector machines (SVM), and k-nearest neighbours (KNN). The supervised learning methods are based on the use of patterns to predict values of labels on unlabelled LULC data. These ways include gradient boosting and regression (Schmitt et al. 2020).

2. Supervised Classification Method Using Support Vector Machines (SVM)

SVM provides a set of high-efficiency algorithms for advanced ML performance (Wu & Shao 2002). The algorithm is a supervised, non-parametric classification method that is able to deal with non-linear classification conditions using a small number of samples (Su et al. 2017; Romaszewski 2016). This algorithm is used to find decision thresholds that improve image class separation based on statistical learning theory principles (Pal & Foody 2010). The SVM classifier has proven to be more efficient in competitive performance with a limited number of training samples, compared to other classifiers currently available (Su et al. 2017). In categorising different classes, SVM is capable of supporting linear and non-linear samples, as well as multiple continuous and discrete samples (Talukdar et al. 2020).

This approach depends on the principle of structural risk minimisation (SRM), by increasing and separates the hyperplane, the data points in closest proximity to the hyperplane, and the data points in closest proximity to the spectral angle mapper (SAM) of the hyperplane, this process can then separate the data points into distinct classes using the spectral hyperplane (Talukdar et al. 2020). During this level, the vectors aim to improve the margin distance between data classes (Pal & Foody 2010; Bouaziz, Eisold & Guermazi 2017). This basically means that the hyperplane is placed right between the closest points of each class. The training samples that specify the hyperplane or margin of the SVM are referred to as support vectors (Shih, Stow & Tsai 2019). The fig (4) illustrates the mechanism of the SVM algorithm (Kumar 2023).

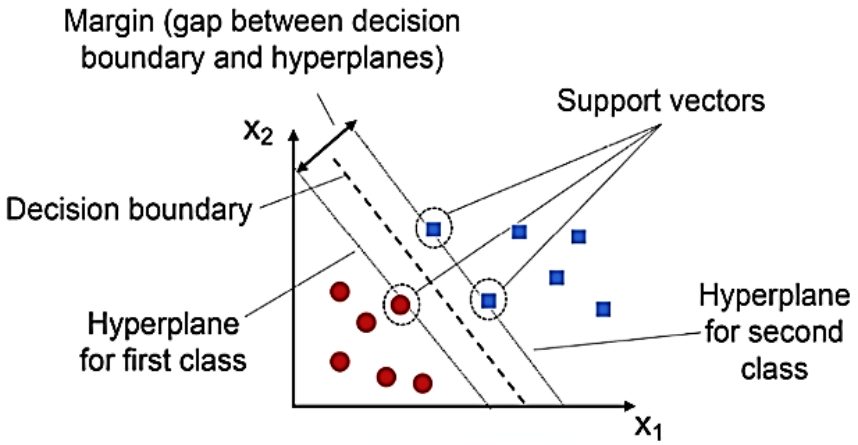

Fig (4). The concept of Support Vector Machine (Kumar 2023).

2.3.2. Training and Validation

The distribution and number of training samples per LULC class were selected according to a deliberate methodology based on the percentage of pixels classified within each category in the satellite image. Table (3). This approach involves the proportional assignment of samples among categories in images, deviating from an equal or random distribution as would be expected under the proportional sampling strategy (Rahman et al. 2022).

In 2000, the total number of samples was 567, which were subsequently divided into classes according to their relative size within the image. The planted/cultivated category had the highest number of pixels (47.11%), with 122 samples assigned to it. while the forest category contained 61 samples and (0.63%) number of pixels, reflecting a relatively high allocation to small classes to ensure spectral discrimination. In 2023, the total number of samples was 488. The category of planted/cultivated comprised 116 samples (51.06%) number of pixels, while

the category of forests included 73 samples (1.17%) number of pixels.

Table 3. Training Sample Counts and Their Pixel-Based Proportions for LULC Classes (2000–2023)

LULC class	2000		2023	
	sample	Pixels%	sample	Pixels%
W	68	3.85	49	4.89
D	50	4.39	112	10.88
B	181	41.01	80	50.89
F	61	0.63	73	1.17
H	85	6.01	58	6.56
P/C	122	47.11	116	51.06
Total	567	103	488	125.45

2.3.3 Accuracy assessment points

Accuracy assessment is one of the basic and final steps in the digital classification process. It aims to verify the objective conformity of the classified image with the reference land cover data, which represents the actual reality (Chuvieco 2016). This is an essential step in assessing the quality of the classification, as it allows for a comparison of the extent to which the classified data corresponds to the actual reference data. Moreover, it helps to identify the error patterns and their sources. In this context, an essential function of the accuracy assessment and error analysis is to provide quantitative comparisons between different land cover explanations, thereby enhancing the reliability of results and providing an objective grounding for comparative analysis.

Validation of the accuracy assessment of the LULC classification was performed using the automated (Compute Confusion Matrix) tool in ArcGIS Pro (Esri 2024). This tool generates key statistical measures, including the user's accuracy (UA) and producer's accuracy (PA). Subsequently, this resulted in the construction of a matrix known as a confusion matrix. This matrix serves as a standard tool to assess classification performance (Srinivas & Narasimha 2011). These indicators are compared to the classification results.

The overall accuracy of the model's performance was calculated by the total correctly classified samples divided by the total number of samples (Raguraman & Bhardwaj 2024) As follows (1):

Overall Accuracy:

$$OA = \frac{TP + TN}{TP + TN + FP + FN} \qquad (1)$$

Where: TP is the True Positive (correctly classified positive samples), TN is the True Negative (correctly classified negative samples), FP is the False Positive (incorrectly classified as positive), and FN is the False Negative (incorrectly classified as negative).

Another image classification accuracy measure used is the Kappa coefficient (K). Its values range from 0 to 1, where the higher the value, the higher the agreement and accuracy (Hasnat 2021; Islam et al. 2021). The Kappa coefficient was calculated automatically with the same tool in the program according to the standard formula (2) (Esri 2024; Lillesand et al. 2015) as follows:

Kappa Coefficient (K):

$$K = \frac{P_o - P_e}{1 - P_e} \qquad (2)$$

where P_o is the observed agreement and P_e the expected agreement by chance.

In this study, a non-traditional approach was adopted in order to obtain the training samples. This approach used high-resolution aerial and satellite imagery and topographic maps obtained from websites such as Copernicus Open Access Hub (Sentinel 2) and Google Earth images rather than relying exclusively on traditional field surveys. The cartographic representations were characterised by an aerial perspective, offering high-resolution imagery with a spatial resolution of 10 metres. The classification's accuracy was verified by representing the investigation points created within the program with a stratified random strategy distributed automatically across all parts of the region. This ensured that no bias was introduced during the investigation. The number of points allocated for each year was 200, with 35 investigation points assigned to each category. The identification of points represented by incorrectly labelled categories was based on the true category value. The values that were entered into the system were separated into two categories: correct and incorrect. The evaluation of each category is based on the absolute values of the number of correct and incorrect samples. This process enables the determination of the performance levels for each classification.

2.4. Monitoring LULC Changes (2000-2023)

The prevailing emphasis in landscape change detection has historically been on the analysis of time series data. However, this study adopted a divergent approach. The study implemented temporal change analysis using the Change Detection Wizard in GIS Pro 3.5 to estimate and analyze the changes that have occurred from the year 2000 to the year 2023 in the study area.

3. Results and Discussion

a. LULC Classification Maps results

The results of the classification and analysis of LULC between 2000 and 2023 reveal clear spatial dynamics. The area of water decreased from 133.8 km² (3.1%) to 55.9 km² (1.2%), indicating a decline in water bodies. Conversely, developed areas exhibited an increase from 150.1 km² (3.5%) to 315.7 km² (7.4%), reflecting substantial urban expansion. Barren area decreased from 1,787.5 km² (42.1%) to 1,484.7 km² (35%), while forest area increased from 148.2 km² (3.5%) to 211.1 km² (5%), reflecting an improvement in vegetation cover. The area of herbaceous decreased from 903.3 km² (21.3%) to 852.5 km² (20.1%), while planted/cultivated increased from 1,125 km² (26.5%) to 1,327.8 km² (31.3%). %). These shifts indicate a marked transition from natural categories (e.g., water and Barren) to anthropogenic ones (e.g., developed areas and agriculture). Table (4), Figs (5 & 6 & 7).

Table 4. Areas (km² &%) of LULC Classes (2000-2023)

LULC Class	2000		2023	
	Area (Km^2)	Area (%)	Area (Km^2)	Area (%)
W	133.8	3.1	55.9	1.2
D	150.1	3.5	315.7	7.4
B	1787.5	42.1	1,484.7	35
F	148.2	3.5	211.4	5
H	903.3	21.3	852.5	20.1
P/C	1125	26.5	1,327.8	31.3
Total	4,248	100	4,248	100

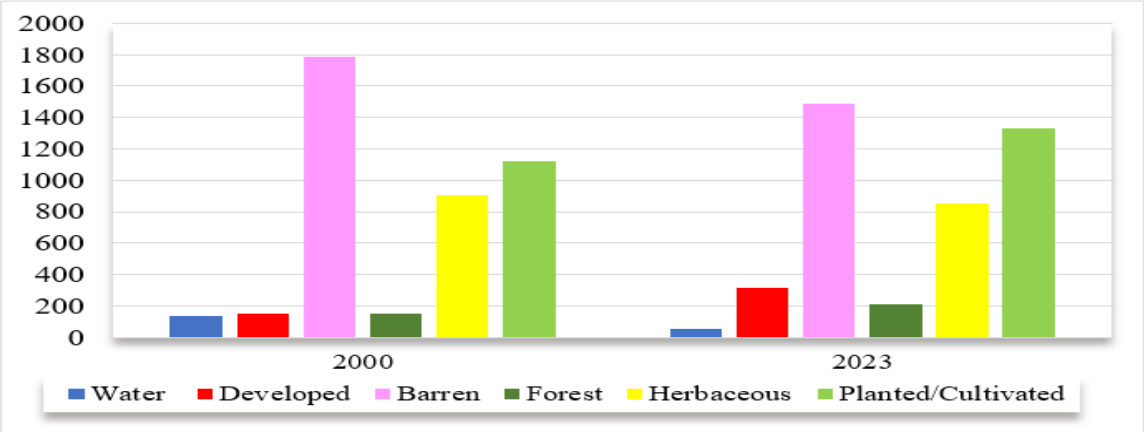

Fig 5. LULC Areas km² (2000-2023)

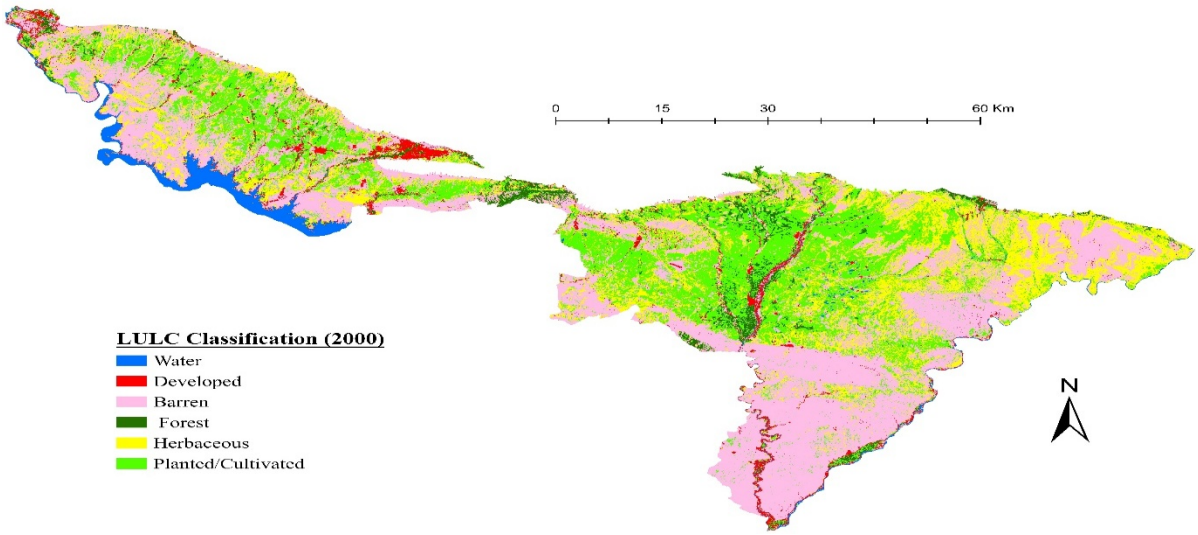

Fig 6. LULC Classification (2000)

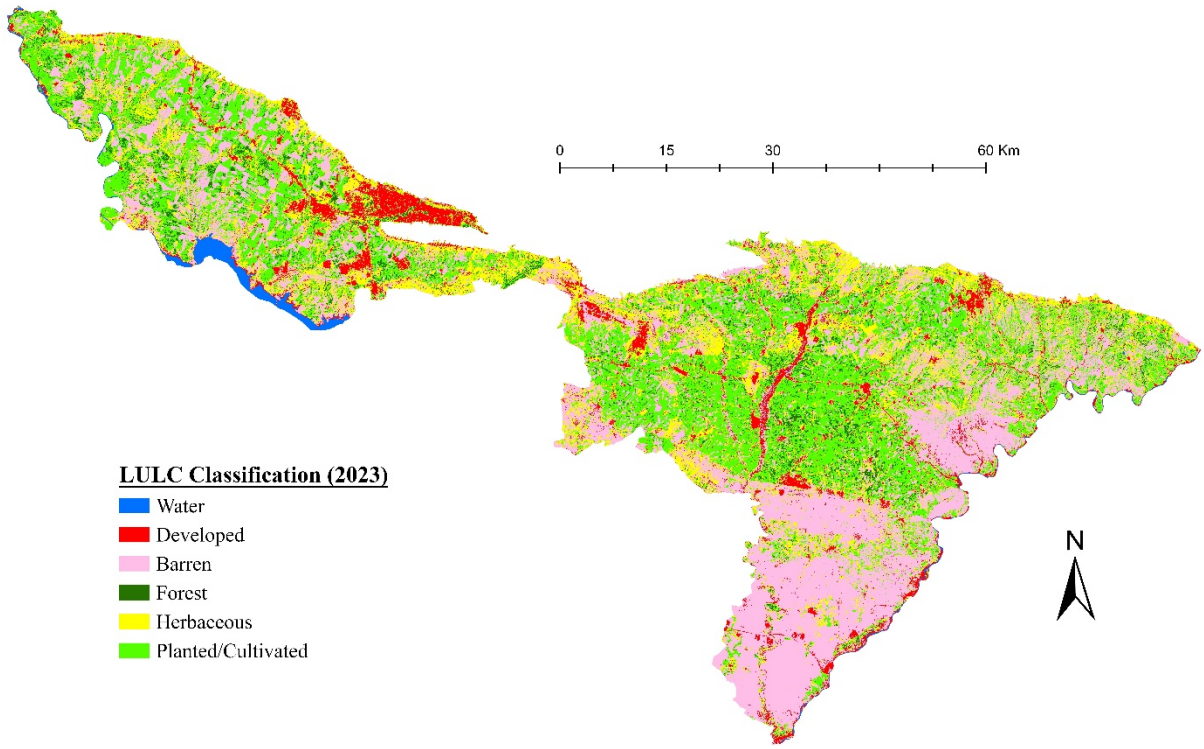

Fig 7. LULC Classification (2023)

b. Accuracy Assessments results

The 2000 error matrix in Table (5) reveals that the model accurately classified water, barren, forest, herbaceous, and planted/cultivated with a complete user accuracy of 1.000, indicating that no classification errors occurred within these categories. Conversely, the developed category demonstrated a user accuracy of 0.800, due to two misclassifications into categories barren and planted/cultivated. Product Accuracy was 1.000 for water, developed, barren, forest, and herbaceous, while planted/cultivated recorded a value of 0.980, reflecting a small percentage of misclassified samples. The overall accuracy for all categories for the year 2000 was 0.9904, while the Kappa coefficient recorded a high value of 0.9868, indicating an almost perfect agreement between the reference classification and the model classification.

In 2023, the results show that the model continues to achieve high classification performance, with classes Water, barren, and planted/cultivated recording a perfect user accuracy of 1.000, while the user accuracy for classes developed, forest, and herbaceous decreased to 0.866667, 0.800, and 0.950, respectively, indicating some instances of misclassification within these classes. Product accuracy for categories Water, developed, barren, forest, and herbaceous was 1.000, while a slight decrease to 0.940 was recorded in planted/cultivated. The overall accuracy for 2023 reached a value of 0.9710, while the Kappa coefficient recorded a value of 0.9609, which is also within the high range, reflecting the quality of classification.

Table 5. Confusion matrix (2000-2023)

Class	W	D	B	F	H	P/C	Total	U_Accuracy	Kappa
					2000				
W	10	0	0	0	0	0	10	1	0
D	0	8	1	0	0	1	10	0.8	0
B	0	0	84	0	0	0	84	1	0
F	0	0	0	10	0	0	10	1	0
H	0	0	0	0	43	0	43	1	0
P/C	0	0	0	0	0	53	53	1	0
Total	10	8	85	10	43	54	210	0	0
P_Accuracy	1	1	0.99	1	1	0.98	0	0.9904	0
Kappa	0	0	0	0	0	0	0	0	0.9868
					2023				
W	10	0	0	0	0	0	10	1	0
D	0	13	2	0	0	0	15	0.866667	0
B	0	0	70	0	0	0	70	1	0
F	0	0	0	8	0	2	10	0.8	0
H	0	0	0	0	38	2	40	0.95	0
P/C	0	0	0	0	0	62	62	1	0
Total	10	13	72	8	38	66	207	0	0
P_Accuracy	1	1	0.97	1	1	0.94	0	0.9710	0
Kappa	0	0	0	0	0	0	0	0	0.9609

c. Change Detection results

The analysis demonstrates that the LULC from 2000 to 2023 for a total area of 4248 km² As illustrated in Table (6), Figs (8 & 9) indicates that the highest rates of change were recorded from herbaceous to planted/cultivated (367.2 km², 8.6%), from barren to herbaceous (346.7 km², 8.2%), and from barren to planted/cultivated (305.4 km², 7.2%), reflecting a clear trend towards intensification of agricultural activity at the expense of natural vegetation cover, which may be related to increased demand for agricultural production or land reclamation policies. The transitions from planted/cultivated to barren land (245.4 km², 5.8%) and from herbaceous to barren land (206.2 km², 4.9%) suggest a potential decline in the quality of agricultural land or environmental shifts that may compromise the sustainability of production. An increase in forest area was recorded, with shifts from other categories into it (such as 57 km², 1.3% from barren land, 56.4 km², 1.3% from herbaceous land, and 82.7 km², 1.9% from planted/cultivated land). However, opposite shifts were also observed, including forest to planted/cultivated (55.3 km², 1.3%) and forest to herbaceous (46.7 km², 1.1%). In contrast, shifts from water bodies were relatively limited, such as water to planted/cultivated (24.1 km², 0.6%) and water to barren (20.9 km², 0.5%), indicating relative stability in this category and limited water bodies in the studied area.

The developed areas exhibited minor reallocations to alternative categories, including developed to barren (35.4 km², 0.8%) and developed to herbaceous (28.3 km², 0.7%). Conversely, the area of land exhibiting no change in land cover during the specified period amounted to 1855.7 km², constituting 43.7% of the total area.

Table 6. Area (km² & %) of LULC changes (2000 -2023)

2000-2023											
	LULCC	km²	%		LULCC	km²	%		LULCC	km²	%
1	W > D	18.5	0.4	12	B > D	118	2.8	23	H > B	206.2	4.9
2	W > B	20.9	0.5	13	B > F	57	1.3	24	H > F	56.4	1.3
3	W > F	2.9	0.1	14	B > H	346.7	8.2	25	H > P/C	367.2	8.6
4	W > H	15.7	0.4	15	B > P/C	305.4	7.2	26	P/C > W	0.6	0
5	W > P/C	24.1	0.6	16	F > W	0.5	0	27	P/C > D	56.7	1.3
6	D > W	1.2	0	17	F > D	11.2	0.3	28	P/C > B	245.4	5.8
7	D > B	35.4	0.8	18	F > B	21.6	0.5	29	P/C > F	82.7	1.9
8	D > F	4	0.1	19	F > H	46.7	1.1	30	P/C > H	191.6	4.5
9	D > H	28.3	0.7	20	F > P/C	55.3	1.3	31	No Change	1855.7	43.7
10	D > P/C	20.1	0.5	21	H > W	0.6	0				
11	B > W	1.5	0	22	H > D	49.8	1.2		**Total**	4,248	100

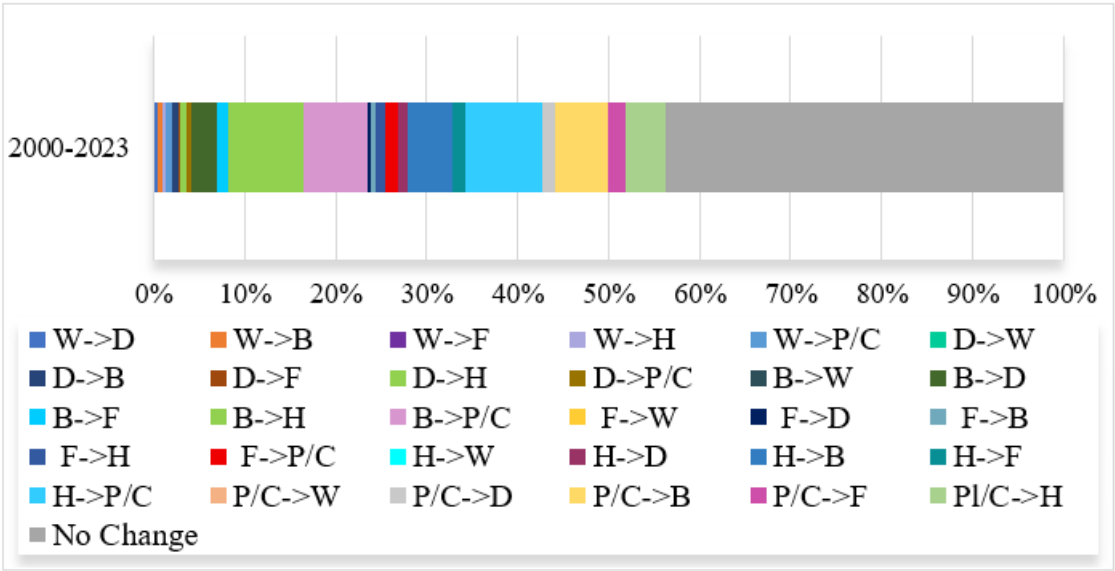

Fig 8. LULC spatiotemporal changes (%) (2000 -2023)

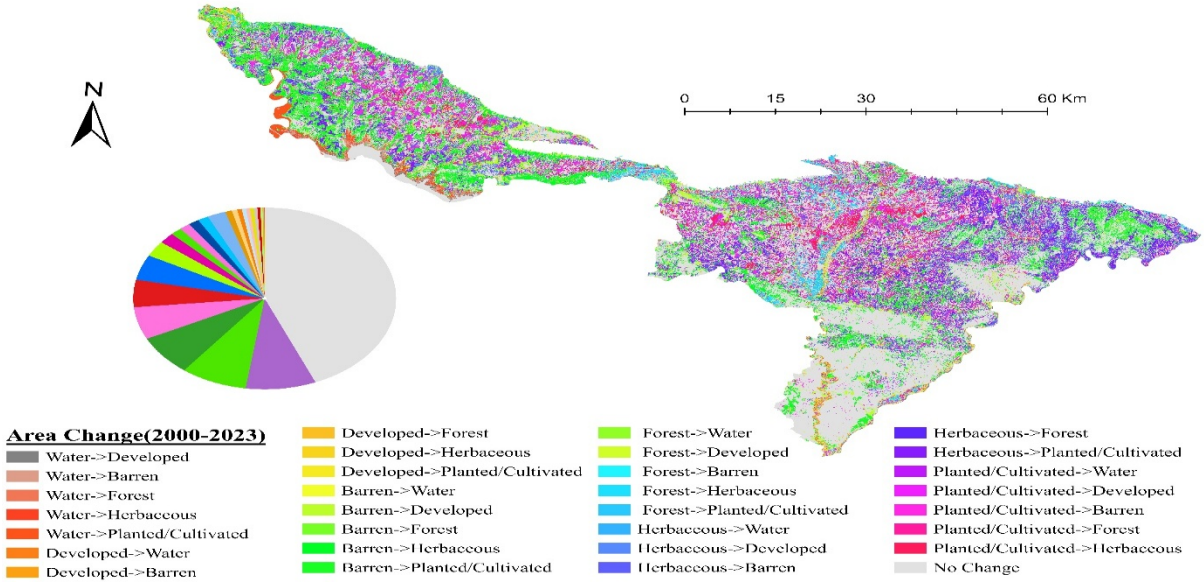

Fig 9. LULC spatiotemporal changes (2000-2023)

4. Discussion

The classification results and the analysis of LULC changes between 2000 and 2023 reveal clear spatial dynamics that reflect the combined influence of human and environmental factors in the study area. The SVM algorithm demonstrated strong classification performance, consistent with findings from previous studies that reported its superiority over other supervised algorithms, including Kernel Logistic Regression (KLR), Naive Bayes Tree (NBT) (Tariq et al. 2023). Artificial Neural Networks (ANN), and Maximum Likelihood Classification (MLC) (Ghayour et al. 2021).

Regarding classification accuracy, the model showed a strong ability to discriminate between LULC classes, particularly those with distinct spectral characteristics. The variation in accuracy between 2000 and 2023 is primarily attributed to differences in image radiometric quality. The 2023 scene exhibited radiometric distortions and atmospheric interference, which reduced spectral separability and consequently lowered classification accuracy. In contrast, the 2000 imagery was clearer and more radiometrically stable, resulting in higher accuracy. This highlights the direct influence of data quality on classification outcomes.

Despite the spectral challenges observed in 2023, classes with strong spectral contrast, such as water bodies, barren land, and planted/cultivated areas, achieved perfect user accuracy (1.000). Conversely, developed areas, forests, and herbaceous categories showed relatively lower accuracy. This reduction is largely due to spectral similarity between certain classes, particularly between developed and planted/cultivated areas, a challenge documented in the literature (Ali & Johnson 2022; Tong et al. 2020). Previous studies have noted that urban surfaces with high reflectance, such as concrete and asphalt, may resemble dry or harvested agricultural fields (Rahman et al. 2020). leading to misclassification when using medium-resolution imagery such as Landsat. These findings underscore the importance of selecting high-quality imagery for future classification applications.

Beyond classification performance, the temporal analysis revealed substantial LULC transformations between 2000 and 2023. The observed shifts indicate a clear trend towards increased agricultural activity, particularly through the conversion of herbaceous and barren land into planted/cultivated areas. This pattern reflects the growing influence of anthropogenic activities, especially agricultural expansion and urban development, on the natural landscape of the study area.

5. Conclusion

This investigation demonstrated the effectiveness of the SVM classifier in analysing LULC changes within the semi-mountainous region of Dohuk Governorate, utilising 30-metre spatial resolution satellite imagery from Landsat 5 and Landsat 8. The SVM algorithm successfully classified the study area into six primary land cover categories, including water bodies, barren land, developed areas, forests, herbaceous, and planted/cultivated land, achieving consistently high classification accuracy across both study years. The model achieved an overall classification accuracy of 0.9904 and a Kappa coefficient of 0.9868 in 2000, and 0.9710 and 0.9609, respectively, in 2023, indicating strong agreement between the reference data and the classification outputs.

The temporal analysis revealed substantial LULC transformations between 2000 and 2023, most notably the expansion of planted/cultivated land and developed areas, accompanied by a marked reduction in barren land. These changes reflect increasing anthropogenic pressures, including agricultural intensification and urban expansion, which are reshaping the natural landscape of the region.

Overall, the findings confirm the suitability of SVM for LULC mapping in complex semi-mountainous environments and highlight the importance of high-quality satellite imagery for achieving reliable classification results. Future research should explore the integration of higher-resolution datasets, multi-temporal imagery, and advanced machine-learning approaches to further enhance classification performance and support sustainable land-use planning in the region.

References

- Abburu, Sunitha, and Suresh Babu Golla. 2015. Satellite Image Classification Methods and Techniques: A Review. International Journal of Computer Applications. 119 (8): 1–6. https://doi.org/10.5120/21088-3779.
- Adam, E., O. Mutanga, J. Odindi, and E. M. Abdel-Rahman. 2014. Land-Use/Cover Classification in a Heterogeneous Coastal Landscape Using Rapid Eye Imagery: Evaluating the Performance of Random Forest and Support Vector Machines Classifiers. International Journal of Remote Sensing. 35 (10): 3440–3458. https://doi.org/10.1080/01431161.2014.903353.
- Alam, Ha-mim Ebne, Md. Nizam Uddin, Kazi Tawkir Ahmed, Md. Jahidul Hasan, Md. Yeasir Arafat, and Md. Enamul Hoque. 2025. "Performance Assessment of Maximum Likelihood, Random Forest and Support Vector Machines Classifier for Urban Land Use Classification: A Case Study of Dhaka Metropolitan City, Bangladesh." Journal of Geospatial Information Science and Engineering 8 (1). https://doi.org/10.22146/jgise.73283.
- Ali, Ahmed, and Mark Johnson. 2022. "Spectral Confusion in Semi-Arid Land Cover Classification: Challenges and Deep Learning Solutions. Sensors, 22 (14): 5123, https://doi.org/10.3390/s22228750.
- Aljanabi, Firas, Mert Dedeoğlu, and Cevdet Şeker. 2024. "Environmental Monitoring of Land Use/Land Cover by Integrating Remote Sensing and Machine Learning Algorithms." Journal of Engineering and Sustainable Development 28 (4): 455–466. https://doi.org/10.31272/jeasd.28.4.4.
- Amini, S., M. Saber, H. Rabiei-Dastjerdi, and S. Homayouni. 2022. Urban Land Use and Land Cover Change Analysis Using Random Forest Classification of Landsat Time Series. Remote Sensing. 14 (11): 2654. https://doi.org/10.3390/rs14112654.
- Anderson, James R. 1971. "Land Use Classification Schemes Used in Selected Recent Geographic Applications of Remote Sensing." Photogrammetric Engineering 27 (4): 379–387.
- Anderson, James R., Ernest E. Hardy, John T. Roach, and Richard E. Witmer. 1976. A Land Use and Land Cover Classification System for Use with Remote Sensor Data. Professional Paper 964. Washington, DC: US Government Printing Office. https://doi.org/10.3133/pp964.
- Aspinall, Richard J., and Michael J. Hill, eds. 2007. Land Use Change: Science, Policy and Management. 1st ed. London: CRC Press. https://doi.org/10.1201/9781420042979.
- Basseville, Michèle. 2009. "Statistical Methods for Change Detection." In Land Use, Land Cover and Soil Sciences – Vol. I, edited by Willy H. Verheye. Oxford: EOLSS Publishers. https://www.eolss.net/Sample-Chapters/C18/E6-43-31-05.pdf.
- Bechtel, B., and C. Daneke. 2012. Classification of Local Climate Zones Based on Multiple Earth Observation Data. IEEE Journal of Selected Topics in Applied Earth Observations and Remote Sensing. 5 (4): 1191–1202. https://doi.org/10.1109/JSTARS.2012.2189873.
- Bhagawat Rimal. 2011. - URBAN GROWTH AND LAND USE/LAND COVER CHANGE OF POKHARA SUB-METROPOLITAN CITY, NEPAL. *Journal of Theoretical and Applied Information Technology* 26 (2).
- Bouaziz, Moncef, Stefanie Eisold, and Emna Guermazi. 2017. Semiautomatic Approach for Land Cover Classification: A Remote Sensing Study for Arid Climate in Southeastern Tunisia, Euro-Mediterranean Journal for Environmental Integration 2 (24). https://doi.org/10.1007/s41207-017-0036-7.
- Chuvieco, Emilio. 2016. Fundamentals of Satellite Remote Sensing: An Environmental Approach. Boca Raton, FL: CRC Press. https://doi.org/10.1201/9780429506482.
- Debebe, Belete, Feyera Senbeta, Ermias Teferi, Dawit Diriba, and Demel Teketay. 2023. 'Analysis of Forest Cover Change and Its Drivers in Biodiversity Hotspot Areas of the Semien Mountains National Park, Northwest Ethiopia'. *Sustainability* 15 (4): 3001. https://doi.org/10.3390/su15043001.
- Esri ArcGIS Pro Documentation – Compute Confusion Matrix (Spatial Analyst), https://pro.arcgis.com/en/pro-app/latest/tool-reference/spatial-analyst/compute-confusion-matrix.htm.
- Fouad, Saffa F. A. 2015. Tectonic Map of Iraq, Scale 1:1000 000, 3rd Edition. Iraqi Bulletin of Geology and Mining. 11 (1): 1–7.
- Gaznayee, Heman Abdulkhaleq A., Ayad M. Fadhil Al-Quraishi, Karrar Mahdi, and Coen Ritsema. 2022. A Geospatial Approach for Analysis of Drought Impacts on Vegetation Cover and Land Surface Temperature in the Kurdistan Region of Iraq. Water. 14 (6): 927. https://doi.org/10.3390/w14060927.
- Ge, G., Z. Shi, Y. Zhu, X. Yang, and Y. Hao. 2020. Land Use/Cover Classification in an Arid Desert-Oasis Mosaic Landscape of China Using Remote Sensed Imagery: Performance Assessment of Four Machine Learning Algorithms. Global Ecology and Conservation. 22: e00971. https://doi.org/10.1016/j.gecco.2020.e00971.
- Ghayour, L., A. Neshat, S. Paryani, H. Shahabi, A. Shirzadi, W. Chen, N. Al-Ansari, M. Geertsema, M. Pourmehdi Amiri, and M. Gholamnia. 2021. Performance Evaluation of Sentinel-2 and Landsat 8 OLI Data for Land Cover/Use Classification Using a Comparison Between Machine Learning Algorithms. Remote Sensing. 13 (7): 1349. https://doi.org/10.3390/rs13071349.
- Ghayour, Laleh, Aminreza Neshat, Sina Paryani, Himan Shahabi, Nadhir Al-Ansari, Marten Geertsema, Ataollah Shirzadi, Mehdi Pourmehdi Amiri, Mehdi Gholamnia, Wei Chen, Jie Dou, and Anuar Ahmad. 2021. Performance Evaluation of Sentinel-2 and Landsat 8 OLI Data for Land Cover/Use Classification Using a Comparison between Machine Learning Algorithms. Remote Sensing 13 (7): 1349. https://doi.org/10.3390/rs13071349.
- Jambally, Mohammed. 2013. "Land Use and Cover Change Assessment Using Remote Sensing and GIS: Dohuk City, Kurdistan, Iraq (1998–2011)." *International Journal of Geomatics and Geosciences* 3 (3): 552–569.

- Jassim, S. Z., and T. Buday. 2006. Units of the Unstable Shelf and the Zagros Suture. In: Geology of Iraq, edited by S. Z. Jassim and J. C. Goff, 71. Prague: Dolin, and Brno: Moravian Museum.
- Kumar, Ajitesh. *Support Vector Machine Explained with Example*. Machine Learning Plus. March 27, 2023. Accessed Jun 18, 2025. https://machinelearningplus.com/machine-learning/support-vector-machine-svm/.
- Liang, J., C. Chen, Y. Song, W. Sun, and G. Yang. 2023. Long-Term Mapping of Land Use and Cover Changes Using Landsat Images on the Google Earth Engine Cloud Platform in Bay Area—A Case Study of Hangzhou Bay, China. Sustainable Horizons. 7: 100061. https://doi.org/10.1016/j.horiz.2023.100061.
- Lunetta, Ross S., David M. Johnson, John G. Lyon, and Jill Crotwell. 2004. Impacts of Imagery Temporal Frequency on Land-Cover Change Detection Monitoring. Remote Sensing of Environment. 89 (4): 444.
- Maxwell, A. E., T. A. Warner, and F. Fang. 2018. Implementation of Machine-Learning Classification in Remote Sensing: An Applied Review. International Journal of Remote Sensing. 39 (9): 2784–2817. https://doi.org/10.1080/01431161.2017.1410301.
- Mzuri, Rebar Tahseen, Abdulla Amir Omar, and Yaseen Taha Mustafa. 2021. Spatiotemporal Analysis of Vegetation Cover and Its Response to Terrain and Climate Factors in Duhok Governorate, Kurdistan Region, Iraq. Iraqi Geological Journal. 54 (1A): 110–126. https://doi.org/10.46717/igj.54.1A.10Ms-2021-01-31.
- OĞUZ, Hakan, Tarq K. Hassan, and Farhad O. Omar. 2025. "The Spatial Analysis of the Terrain Impact on Agricultural Land Use by Using GIS and RS Techniques: A Case Study of Soran District-Erbil-Iraq." ZANCO Journal of Pure and Applied Sciences. 24 (6): 269–289. https://doi.org/10.21271/zjhs.24.6.20.
- Pal, Mahesh, and Giles M. Foody. 2010. Feature Selection for Classification of Hyperspectral Data by SVM. IEEE Transactions on Geoscience and Remote Sensing. 48 (5): 2297–2307. https://doi.org/10.1109/TGRS.2009.2039484
- Raguraman, Naren, and Ashutosh Bhardwaj. 2024. Spatial Analysis of Land Use Land Cover Dynamics in the Madurai District Using Sentinel-2 Data and Supervised Learning Algorithms. In The International Archives of the Photogrammetry, Remote Sensing and Spatial Information Sciences, XLVIII-4-2024, 367–372. ISPRS TC IV Mid-term Symposium, Spatial Information to Empower the Metaverse, Fremantle, Perth, Australia, October 22–25, 2024. https://doi.org/10.5194/isprs-archives-XLVIII-4-2024-367-2024
- Rahman, A., Abdullah, H. M., Tanzir, M. T., Hossain, M. J., Khan, B. M., Miah, M. G., and Islam, I. 2020. Performance of Different Machine Learning Algorithms on Satellite Image Classification in Rural and Urban Setup. Remote Sensing Applications: Society and Environment 20: 100410. https://doi.org/10.1016/j.rsase.2020.100410
- Rahman, Md. M., Tabash, M. I., Salamzadeh, A., Abduli, S., & Rahaman, Md. S. 2022. Sampling Techniques (Probability) for Quantitative Social Science Researchers: A Conceptual Guidelines with Examples. *SEEU Review*, *17*(1), 42–51. https://doi.org/10.2478/seeur-2022-0023
- Romaszewski, Michał, Przemysław Głomb, and Michał Cholewa. 2016. Semi-Supervised Hyperspectral Classification from a Small Number of Training Samples Using a Co-Training Approach. ISPRS Journal of Photogrammetry and Remote Sensing. 121: 60–76. https://doi.org/10.1016/j.isprsjprs.2016.08.011.
- Schmitt, M., J. Prexl, P. Ebel, L. Liebel, and X. X. Zhu. 2020. Weakly Supervised Semantic Segmentation of Satellite Images for Land Cover Mapping—Challenges and Opportunities. ISPRS Annals of the Photogrammetry, Remote Sensing and Spatial Information Sciences. V-3-2020: 795–802. https://doi.org/10.5194/isprs-annals-V-3-2020-795-2020.
- Shih, Hsiao-Chien, Douglas A. Stow, and Yu Hsin Tsai. 2019. Guidance on and Comparison of Machine Learning Classifiers for Landsat-Based Land Cover and Land Use Mapping, International Journal of Remote Sensing, 40 (4): 1248–1274. https://doi.org/10.1080/01431161.2018.1524179.
- Sreenivasa, K. R., and Roddam Narasimha. 2011. Laboratory Simulations Show Diabatic Heating Drives Cumulus-Cloud Evolution and Entrainment." Proceedings of the National Academy of Sciences of the United States of America. 108 (30): 12300–12304. https://doi.org/10.1073/pnas.1112281108
- Su, Yiting, Xingguang Yan, Jing Li, Andy Smith, Di Yang, and Tianyue Ma. 2017. Rapid Land Cover Classification Using a 36-Year Time Series of Multi-Source Remote Sensing Data. Land 12 (12): 2149. https://doi.org/10.3390/land12122149
- Talukdar, Swapan, Pankaj Singha, Susanta Mahato, Shahfahad, Yuei-An Liou, and Atiqur Rahman. 2020. Land-Use Land-Cover Classification by Machine Learning Classifiers for Satellite Observations-A Review, Remote Sensing, 12 (7): 1135. https://doi.org/10.3390/rs12071135.
- Tarabalka, Y., J. Benediktsson, and J. Chanussot. 2009. Spectral-Spatial Classification of Hyperspectral Imagery Based on Partitional Clustering Techniques. IEEE Transactions on Geoscience and Remote Sensing 47 (8): 2973–2987.
- Tariq, Aqil, Yan Jiango, Walid Soufan, Qingting Li, Khalid F. Almutairi, Jianwei Gao, Linlin Lu, and Muhammad Habib-ur-Rahman. 2023. Modelling, Mapping and Monitoring of Forest Cover Changes, Using Support Vector Machine, Kernel Logistic Regression and Naive Bayes Tree Models with Optical Remote Sensing Data. Heliyon 9: e13212.https://doi.org/10.1016/j.heliyon.2023.e13212.
- Thanh Noi, P., and M. Kappas. 2017. Comparison of Random Forest, k-Nearest Neighbor, and Support Vector Machine Classifiers for Land Cover Classification Using Sentinel-2 Imagery. Sensors. 17 (18): 452. https://doi.org/10.3390/s17020452.
- Tong, Xin-Yi, Gui-Song Xia, Qikai Lu, Huanfeng Shen, Shengyang Li, Shucheng You, and Liangpei Zhang. 2020. "Land-Cover Classification with High-Resolution Remote Sensing Images Using Transferable Deep Models." ISPRS Journal of Photogrammetry and Remote Sensing, 158: 279–293. https://doi.org/10.1016/j.rse.2019.111322.
- UN-Habitat. 2020. *Annual Report 2020*. Nairobi: United Nations Human Settlements Programme. https://unhabitat.org/annualreport

- Wu, Qiang, Li Zhang, and Xiaohui Li. 2025. “Improving Land Cover Classification Accuracy by Integrating Spectral and Spatial Features.” PLOS One, 20 (3): e0281234.
- Wu, W., & Shao, G., 2002, Optimal combinations of data, classifiers, and sampling methods for accuracy assessment of land cover classification. *Canadian Journal of Remote Sensing*, *28*(4), 601–609.
- Xia, J., J. Chanussot, P. Du, and X. He. 2014. Semi-Supervised Probabilistic Principal Component Analysis for Hyperspectral Remote Sensing Image Classification. IEEE Journal of Selected Topics in Applied Earth Observations and Remote Sensing 7 (6): 2224–2236.
- Zhang, C., and X. Li. 2022. Land Use and Land Cover Mapping in the Era of Big Data. Land 11 (1692). https://doi.org/10.3390/land11101692.
- Zhang, L., L. Zhang, D. Tao, and X. Huang. 2012. On Combining Multiple Features for Hyperspectral Remote Sensing Image Classification. IEEE Transactions on Geoscience and Remote Sensing 50 (3): 879–893.

چاوەڕوانکردنی گۆڕانکارییەکانی بەکارهێنانی زەوی و ڕووپۆشی زەوی لە ناوچەی نیمچە شاخاوی پارێزگای دهۆک بە بەکارهێنانی وێنەی لاندسات وئامێری ڤێکتەری پشتگیری (SVM)

داستان فەتحی ئەحمەد

بەشە جۆرافیا، کۆلێژی زانستە مرۆییەکان،زانکۆی دهوک، هەرێمی کوردستان، عێراق

dastan.fa6323@stu.uod.ac

نشوان شکری عەبدوللا

بەشە جۆرافیا، کۆلێژی زانستە مرۆییەکان،زانکۆی دهوک، هەرێمی کوردستان، عێراق

nashwan.shukri@uod.ac

پوختە

ئەم توێژینەوەیە گۆڕانکارییە درێژخایەنەکانی بەکارهێنانی زەوی و ڕووپۆشی زەوی لە ناوچەی نیمچە شاخاوی پارێزگای دهۆک لە هەرێمی کوردستانی عێراق لە ماوەی 2000-2023 شیکاری دەکات، بە بەکارهێنانی وێنەی مانگی دەستکردی لاندسات Landsat 5 TM و OL 8 و تەکنیکەکانی پۆلێنکردنی فێربوونی ئامێر (ML). ناوچەی لێکۆڵینەوەکە زەوییەکی چەقۆی تێدایە کە فەلات و دەشتە کشتوکاڵییەکان تێکەڵ دەکات. ئەمەش تەحەدای سپێکترالّ لە جیاکردنەوەی نێوان چینە زەوییە هاوشێوەکان دروست دەکات و دەیکاتە مۆدێلێکی ئایدیاڵ بۆ تاقیکردنەوەی کاریگەری ئەلگۆریتمەکانی فێربوونی ئامێر لە ژینگە ئاڵۆزەکاندا.

پۆلێنکردنی ئاڕاستەکراو بە بەکارهێنانی ئەلگۆریتمێکی ئامێری ڤێکتەری پشتگیری (SVM) لە GIS Pro 3.5 جێبەجێ کرا. ئەنجامەکان گۆڕانکارییەکی بەرچاویان لە شێوازی ڕووپۆشکردنی زەویدا دەرخست، کە ڕووبەری زەوییە گەشەسەندووەکان لە 3.5% بۆ 7.4% زیادیکردووە، لەکاتێکدا ڕووبەری زەوییە ڕووتەکان لە 42.1% بۆ 35% کەمیکردووە. هەروەها ڕووبەری کشتوکاڵی/کێڵگراو لە 26.5% بۆ 31.3% زیادی کردووە. وردی پۆلێنکردن بە گشتی 99.04% بۆ ساڵی 2000 و 97.10% بۆ ساڵی 2023 بووە، لەگەڵ بەهاکانی کاپا (Kappa) بە ڕێککەوت 0.9868 و 0.9609، کە ئاماژەیە بۆ کارایی پۆلێنکردنێکی بەرز.

هەروەها توێژینەوەکە گۆڕانکارییە ژینگەییەکانی بەرچاوی ئاشکرا کردووە، دیارترینیان گواستنەوەی ڕووبەرە بەرفراوانەکانی زەوییە بێ بەرهەمەکانە بۆ ناوچە کشتوکاڵییەکان/چێنراوەکان و گیاییەکان، کە ڕەنگدانەوەی کاریگەرییەکانی فراوانبوونی شارەکان و ئیستغلالکردنی ناپایەدارە لە سەرچاوەکانی زەوی.

وشە سەرەکییەکان: سیستەمی زانیاری جوگرافی (GIS)؛ بەکارهێنانی زەوی/ڕووپۆشی زەوی (LULC)؛ هەستکردن لە دوورەوە (RS)؛ فێربوونی ئامێر (ML)؛ ئامێری ڤێکتەری پشتگیری (SVM)

رصد تغيرات الاستعمال الأرضي والغطاء الارضي في المنطقة شبه الجبلية في محافظة دهوك بتوظيف صور لاندسات وآلة المتجهات الدعمة (SVM)

داستان فتحي أحمد

قسم الجغرافيا، كلية العلوم الإنسانية، جامعة دهوك,دهوك، إقليم كردستان، العراق

dastan.fa6323@stu.uod.ac

نشوان شكري عبد الله

قسم الجغرافيا، كلية العلوم الإنسانية، جامعة دهوك,دهوك، إقليم كردستان، العراق

nashwan.shukri@uod.ac

الملخص

تحلل هذه الدراسة التغيرات طويلة الامد في استخدام الأراضي والغطاء الأرضي في المنطقة شبه الجبلية من محافظة دهوك في اقليم كوردستان العراق خلال الفترة 2000–2023، باستخدام صور الأقمار الصناعية Landsat 5 TM وOL8 ، وتقنيات تصنيف التعلم الآلي (ML). تتميز تضاريس منطقة الدراسة بتضاريس متداخلة تجمع بين الهضاب والسهول الزراعية. وهذا يخلق تحديات طيفية في التمييز بين فئات الأراضي المتشابهة ويجعلها نموذجًا مثاليًا لاختبار فعالية خوارزميات التعلم الآلي في البيئات المعقدة.

تم تطبيق التصنيف الموجّه باستخدام خوارزمية آلة دعم المتجهات (SVM)ضمن بيئة نظام المعلومات الجغرافية GIS Pro 3.5. أظهرت النتائج تغيرات كبيرة في أنماط الغطاء الأرضي، حيث ارتفعت مساحة الأراضي المطورة من 3.5% إلى 7.4%، بينما انخفضت مساحة الأراضي الجرداء من 42.1% إلى 35%. كما زادت مساحة المزروعة/المحروثة من 26.5% إلى 31.3%. وبلغت الدقة الإجمالية للتصنيف 99.04% لعام 2000 و97.10% لعام 2023، وبلغت قيمتي Kappa 0.9868 و0.9609 على التوالي، مما يشير إلى كفاءة تصنيف عالية.

كما كشفت الدراسة أيضاً عن تغيرات بيئية كبيرة، أبرزها انتقال مساحات كبيرة من الأراضي الجرداء إلى فئات مزروعة/المحروثة وعشبية مما يعكس آثار التوسع العمراني والاستغلال غير المستدام لموارد الأراضي.

الكلمات المفتاحية: نظم المعلومات الجغرافية (GIS)؛ استخدام الأراضي/الغطاء الأرضي (LULC)؛ الاستشعار عن بعد (RS)؛ التعلم الآلي (ML)؛ آلة دعم المتجهات (SVM).